Virchows Arch (2009) 455:323–336
DOI 10.1007/s00428-009-0837-4

ORIGINAL ARTICLE

Nodular pattern of bone marrow infiltration: frequent finding in immunosuppression-related EBV-associated large B-cell lymphomas

Deborah W. Sevilla · Erin M. Weeden · Suzy Alexander · Vundavalli V. Murty · Bachir Alobeid · Govind Bhagat

Received: 30 June 2009 / Revised: 29 August 2009 / Accepted: 14 September 2009 / Published online: 6 October 2009

Abstract Different patterns of bone marrow (BM) infiltration by diffuse large B cell lymphomas (DLBCL) have been described. A pure nodular pattern is uncommon, and the pathologic features, as well as the clinical correlates of DLBCL manifesting this pattern in the BM have not been well characterized. We evaluated BM biopsies involved by large B cell lymphomas diagnosed at our institute over an 11-year period to assess the morphology, phenotype, cytogenetic abnormalities, and clinical features of cases associated with a nodular pattern. A distinct nodular pattern of BM involvement was noted in 14 out of 55 (25%) cases. Although both EBV+ and EBV− DLBCL with this pattern were identified, a pure nodular pattern was significantly more common in EBV+ DLBCL compared to EBV− DLBCL (8/9, 89% versus 6/46, 13%; P=0.00002). The majority of EBV+ DLBCL associated with a nodular pattern had distinctive morphologic features (polymorphic cellular infiltrate and pleomorphic cytology), and CD30 expression was more commonly observed in this group (P=0.0163). All EBV+ DLBCL and two out of six (33%) EBV− DLBCL had nongerminal center phenotypes. No recurrent cytogenetic abnormalities were detected in either group. Importantly, all EBV+ DLBCL occurred in individuals with immune dysfunction (organ transplant recipients, HIV infection) or in those >50 years of age. Our study indicates a much higher predilection for EBV+ DLBCL to involve the marrow in a nodular pattern compared to EBV− cases and highlights similarities in the morphologic pattern of BM involvement by previously recognized subsets of immunodeficiency-related EBV+lymphomas and the newer entity of "EBV+ DLBCL of the elderly."

Keywords Diffuse large B cell lymphoma · Epstein–Barr virus · Bone marrow · Nodular pattern

D. W. Sevilla · E. M. Weeden · S. Alexander · V. V. Murty · B. Alobeid · G. Bhagat
Department of Pathology, Columbia University Medical Center, New York Presbyterian Hospital, 630 W. 168th Street, 14th Floor, New York, New York 10032, USA

G. Bhagat (✉)
Department of Pathology, College of Physicians and Surgeons, Columbia University, 630 West 168th Street, Vanderbilt Clinic Room 14-228, New York, New York 10032, USA
e-mail: gb96@columbia.edu

Introduction

Bone marrow (BM) examination is an integral part of the Ann Arbor staging system for B cell non-Hodgkin lymphomas (B-NHL). Bone marrow involvement indicates stage IV disease, which is an adverse prognostic factor in the International Prognostic Index (IPI), but it is also independently associated with a worse prognosis [1]. The frequency of BM involvement by B-NHL varies according to disease subtype. Marrow infiltration is more commonly observed in patients with low grade B-NHL, ranging from 30% for marginal zone lymphomas to virtually 100% for chronic lymphocytic leukemias [2–7], compared to diffuse large B cell lymphomas (DLBCL; 8–35%) [2, 3, 8–13]. Differences in the frequency of BM involvement by DLBCL, with regard to their phenotype or association with Epstein–Barr virus (EBV) infection, are currently unclear. Characteristic patterns of BM infiltration by different subtypes of B-NHL have also been reported, with the paratrabecular pattern more commonly seen in follicular lymphoma, the interstitial

diffuse and/or nodular pattern frequently observed in chronic lymphocytic leukemia/small lymphocytic lymphoma and lymphoplasmacytic lymphoma, and the sinusoidal pattern most often associated with splenic marginal zone lymphoma [2, 14, 15]. Only a few studies have described different patterns of BM involvement by DLBCL [2, 6, 16]. These include diffuse, interstitial, paratrabecular, nodular, and mixed patterns. A pure nodular pattern appears to be one of the least common, observed in 0–23% of cases [2, 4–6, 16], and DLBCL manifesting this pattern of BM infiltration have not been well-characterized. Thus, we undertook this study to assess the morphology, phenotype, associated cytogenetic abnormalities, and clinical features of DLBCL with a distinct nodular pattern of BM involvement. We observed nodular BM infiltrates in both EBV− and EBV+ DLBCL; however, this pattern was significantly more common in EBV+ DLBCL. All of the EBV+ DLBCL in our series occurred in immunosuppressed patients and included cases representing the recently described entity of EBV+ DLBCL of the elderly.

Methods

Case selection and clinical characteristics

A search of our departmental database was performed to identify BM biopsies, which had infiltrates of DLBCL over a period of 11 years (January 1997–December 2007). Morphologic features were assessed using H&E stained sections of Bouin's fixed paraffin-embedded BM biopsies. The pattern of BM involvement was analyzed to identify cases with pure nodular infiltrates of DLBCL. A distinct or pure nodular pattern was defined as the presence of well-delineated or circumscribed aggregates of large neoplastic lymphocytes with <10% of the neoplastic cells demonstrating a different pattern of infiltration (i.e., single scattered cells) [2]. The corresponding formalin-fixed paraffin-embedded lymph node (LN) or soft tissue biopsies of the DLBCL, where available, were also evaluated to characterize architectural and cytologic features.

Data regarding patient demographics, EBV viral load and/or serology, immune status, immunosuppressive regimen, chemotherapy and/or radiation therapy, and clinical outcomes were obtained from our laboratory information system. Epstein–Barr virus reactivation was defined as detection of >100 copies per milliliter of EBV antigen by polymerase chain reaction (PCR) analysis.

Immunohistochemistry and in situ hybridization

Immunohistochemical stains were performed on the BM biopsies and LN or soft tissue biopsies, using the primary antibodies listed in Table 1, after heat-induced antigen retrieval, and were visualized with Envision plus (DAKO, Carpinteria, California, USA) and DAB. Cases were scored as positive for the antigen of interest if >30% of the neoplastic cells expressed it. Based on the expression of CD10, BCL6, and IRF4, the DLBCL were classified as either germinal center (GC) type (CD10+ or CD10−/BCL6+/IRF4−) or non-GC type (CD10−/BCL6+/ IRF4+ or CD10−/BCL6−/IRF4+) [17]. Semiquantitative assessment of the reactive T cells within the nodules of DLBCL was performed on CD3-stained sections (<10%=mild, >10–50%=moderate, >50%=marked).

In situ hybridization for EBV-encoded small RNAs (EBER) was performed using the supplied protocol (INFORM EBER, Ventana, Tuscon, Arizona, USA). Cases were considered EBV+ when the vast majority (>90%) of neoplastic cells expressing one or more of the B cell antigens (CD20/PAX5/OCT2) demonstrated a positive signal by EBER.

Cytogenetic analysis

Giemsa banding was performed on metaphase preparations obtained after short term (12 h) unstimulated cultures of the BM aspirate, LN, or soft tissue biopsies using standard methods. Karyotypes were described according to the International System for Human Cytogenetic Nomenclature [18]. Fluorescence in situ hybridization (FISH) was performed on methanol/acetic acid fixed cells using immunoglobulin heavy chain gene (*IGH*), *BCL6*(3q27), and *c-MYC*(8q24) dual color break-apart probes (VYSIS, Downers Grove, Illinois, USA) or locus specific probes for *TP53/ATM* (VYSIS) and *BLIMP1*(*PRDM1*)(6q21) [19], as indicated, according to standard protocols. Fluorescence signals were captured after analyzing 200–300 cells and counterstaining with DAPI using the Cytovision Imaging system attached to a Nikon Eclipse 600 microscope (Applied Imaging, Santa Clara, California, USA).

Immunoglobulin heavy chain gene rearrangement

Polymerase chain reaction analysis to detect *IGH* variable region gene rearrangement was performed on bone marrow aspirates and LN or soft tissue biopsies, using the Biomed-2 primers (IVS Gene Clonality Assay Kit, InVivo Scribe Technologies, San Diego, CA, USA).

Statistical analysis

The observed data were tested for normalcy using a Kolmogorov–Smirnov test. Statistical significance of differences between groups was calculated using the one-tailed Student's *t* test with a significance threshold of $P<0.001$ or

Table 1 Immunohistochemical staining profile of DLBCL with a nodular pattern of bone marrow infiltration

Antibody, clone, company	EBV+ (n=8)						EBV− (n=6)							
Case number	1	2	3	4	5	6	7	8	9	10	11	12	13	14
CD45, 2B11+PD7/26, DAKO, Carpinteria, California, USA	+	+	+	+	+	+	+	+	+	+	+	+	+	+
CD20, L26, DAKO	−	+	+	+	+	+	+	+	+	+	+	+	+	+
PAX5, 24, Cell Marque, Rocklin, California, USA	−	+	+	+	+	+	+	+	+	+	+	+	+	+
CD79a, JCB117, DAKO	+	+	+	+	+	+	+	+	+	+	+	+	+	+
Pu-1, G148-74, BDPharm, Franklin Lakes, New Jersey	+	+	+	−	−	+	+	−	+	+	+	+	+	+
OCT2, N/A, Santa Cruz	+	+	+	+	+	+	+	+	+	+	+	+	+	+
CD10, Calla (56C6), Novacastra, Newcastle upon Tyne, UK	−	−	−	−	−	−	−	−	+	−	−	−	+	−
BCL6, PG-B6P, DAKO	−	+	−	−	+	+	−	−	+	+	−	+	+	+
IRF4, MUM1p, DAKO	+	+	+	+	+	+	+	+	−	−	+	−	−	+
CD138, M115, DAKO														
CD30, Ber-H2, DAKO	+	−	+	+	+	+	+	+	−	−	−	−	−	+
BCL2, 124, DAKO	+	−	−	+	+	+	+	+	+	+	+	+	+	+
CD15, LEUM1, DAKO	−	−	−	−	−	−	−	−	−	−	−	−	−	−
CD5, CD5/54/P6, DAKO	−	−	−	−	−	−	−	−	−	−	−	−	−	−
Fascin, 55 K2, DAKO	−	−	+	−	−	−	−	−	−	−	−	−	−	−
p53[a], BP53-12-1, BIOGENEX, San Ramon, California, USA	+	−	−	−	−	−	−	−	−	+	−	−	−	+
Ki-67[b], MIB1, DAKO	90	80	80	50	80	60	90	70	30	90	50	60	70	80
HHV8 (LANA), 13B10, Cell Marque	−	−	−	−	−	−	−	−	−	−	−	−	−	−
EBNA2, PE2, DAKO	−	+	−	−	−	+	−	−	−	−	−	−	−	−
LMP1, CSI-4DAKO	+	+	+	+	+	+	+	+	−	−	−	−	−	−
EBER, in situ hybridization; Ventana, Tucson, Arizona, USA	+	+	+	+	+	+	+	+	−	−	−	−	−	−
CD3[c], F7.2.38, DAKO	1	1	2	1	2	1	3	3	1	1	2	1	3	1
CD4:CD8[d]CD4, SP35, Cell Marque CD8, C8/144B, DAKO	1:10	1:2	1:2	1:7	1:2	1:3	1:1	1:2	1:2	1:2	1:1	1:2	1:2	1:1

[a] p53 considered positive if >30% of the neoplastic cells demonstrated nuclear expression

[b] Ki-67 expressed as percentage of neoplastic cells

[c] CD3 staining profile refers to nonneoplastic T cells within the nodules, 1=mild, 2=moderate, and 3=marked

[d] CD4:CD8 ratio refers to relative proportions of reactive T cells within the nodules

Fisher's exact probability test, and a P value of <0.05 was considered significant.

Results

Case and patient characteristics

Fifty-five cases of DLBCL involving the BM were diagnosed at our institute during the study period, and the most common primary pattern of BM involvement was diffuse (23/55, 42%), followed by nodular (18/55, 32%), interstitial single-cell (12/55, 22%), and paratrabecular (2/55, 4%). Of the 18 cases with a nodular component, four were eliminated since they exhibited a mixed pattern and did not fulfill our definitional criteria (three had a component of diffuse infiltrate and one had numerous single scattered cells). Thus, 14 of 55 (25%) BM biopsies exhibited a pure nodular pattern. In all, except one case, besides the nodular aggregates, the minor component of single scattered or small clusters of neoplastic cells, represented <5% of the DLBCL infiltrate; one case had an additional component of scattered neoplastic cells approaching 10% of the total DLBCL infiltrate. EBV− DLBCL with a nodular pattern accounted for six of 46 of all EBV− cases (13%), whereas EBV+ DLBCL with a nodular pattern represented eight of nine (89%) of all EBV+ cases involving the BM (P=0.00001967868), only one EBV+ DLBCL with a non-nodular pattern (single cell interstitial infiltrate) was seen in our series.

Clinical characteristics of the patients are described in Table 2. All patients presented with de novo DLBCL, except one patient with an EBV+ DLBCL who had a history of B-NHL, not otherwise specified, 14 years prior to the current BM biopsy. The morphology was identical in the previous BM biopsy; however, no material was available to perform in situ hybridization for EBER in the prior biopsy. A male predominance was observed for EBV+ DLBCL (M:F=5:3), while patients with EBV− DLBCL had an equal gender distribution (M:F=3:3). There was no significant difference in the median age of patients that had EBV+ or EBV− DLBCL (66 years versus 59 years, range 3–83 years and 34–84 years, respectively; P=0.4192). Additionally, no difference in the mean age of patients with EBV− nodular DLBCL, and those that had EBV− DLBCL with other patterns of BM involvement was noted. No significant difference in lactate dehydrogenase (LDH) levels, IPI, Eastern Cooperative Oncology Group (ECOG) performance status, or response rates was seen between the two groups. EBV+ DLBCL with a nodular pattern were seen exclusively in immunocompromised patients: HIV+ (n=2), solid organ transplant (n=3), and old age (>50 years, n=3); two of the recipients of solid organ transplants were >50 years of age, while five of six (83%) individuals with EBV− nodular DLBCL were >50 years of age, but none of the latter had any apparent immune dysfunction. None of the patients had a concurrent (or prior) T cell lymphoma or an autoimmune or collagen vascular disease, and with the exception of PTLD patients, none received immunosuppressive medication (e.g. methotrexate).

At diagnosis, PCR-based EBV viral load assessment was performed in five of eight patients with EBV+ DLBCL and in two of six patients with EBV− DLBCL. An elevated serum EBV viral load was noted at the time of diagnosis in all five EBV+ DLBCL (range 411,000–1,352,000 copies per milliliter; mean 852,000). Epstein–Barr virus was undetectable on follow-up evaluation in two of the five cases, both PTLD patients (1 month and 1 year after diagnosis). None of the tested EBV− cases had measurable viral loads at the time of diagnosis.

Morphology and phenotype

The nodules in all eight EBV+ DLBCL were discrete and had rounded contours, with numerous admixed histiocytes, small lymphocytes, occasional plasma cells, and variable numbers of neoplastic cells (Fig. 1). Histiocyte-rich nodules (highlighted with a stain for PGM-1), with histiocytes comprising >50% of the nodule cellularity, were seen in five of eight (62%) cases. The nodules varied in size, both within the same biopsy and between different biopsies, ranging from small (nodules occupying ≤1/2 of a high power field, 400×) to large and expansile (nodules occupying at least one high power field; Table 3). BM biopsies in three of eight cases (38%) showed only interstitial nodules, and only paratrabecular nodules were seen in three cases (38%); two (25%) had both paratrabecular and interstitial nodules (Table 3). A single case showed one nodule in which the neoplastic cells displayed an angiocentric pattern with accompanying coagulative necrosis (Fig. 2f); while in three cases, the nodules had single-scattered apoptotic cells. Neoplastic cells were quantified based on CD20, PAX5 and/or OCT2 staining as assessment of H&E stained slides always underestimated the number of neoplastic cells. In the majority of biopsies (5/8, 62%), large neoplastic cells comprised a minority of the cellular elements (20–30%) that were either seen as scattered cells at the periphery (targetoid pattern) or randomly distributed throughout the nodules (Fig. 3). In the remaining cases (3/8, 38%), neoplastic cells comprised >30% of the nodular cellular infiltrate (Fig. 2h). The neoplastic cells had centroblastic morphology (large lymphocytes with scant to moderate amphophilic cytoplasm, round to ovoid nuclear contours, fine chromatin, and multiple small nucleoli) in only two of eight (25%) cases (Fig. 2h), with the majority (6/8, 75%) displaying pleomorphic cytologic features (large lymphocytes with angulated or irregular nuclear contours) and bizarre or Reed–Sternberg (RS)-like cells were identified in four (66%) of the latter biopsies (Fig. 2d).

Table 2 Clinical characteristics of patients with nodular infiltration of bone marrow by DLBCL

Variables	EBV+ cases (n=8)	EBV− cases (n=6)
Sex (male/female)	5/3	3/3
Age, median (range; years)	66 (3–83)	59 (34–84)
Older than 60	6 (75%)[a]	3 (50%)[a]
ECOG PS 2–4	3 (38%)[a]	1 (17%)[a]
Bsymptoms, presence	6 (75%)[a]	3 (50%)[a]
LDH elevated	8 (100%)[a]	6 (100%)[a]
Ann Arbor stage III/IV	8 (100%)[a]	6 (100%)[a]
Extranodal involvement (>1 site)	4 (50%)[a]	2 (33%)[a]
IPI,high intermediate/high	6 (75%)[a]	4 (66%)[a]

ECOG Eastern Cooperative Oncology Group, *PS* performance status, *LDH* lactate dehydrogenase, *IPI* International Prognostic Index

[a] Number of cases (%)

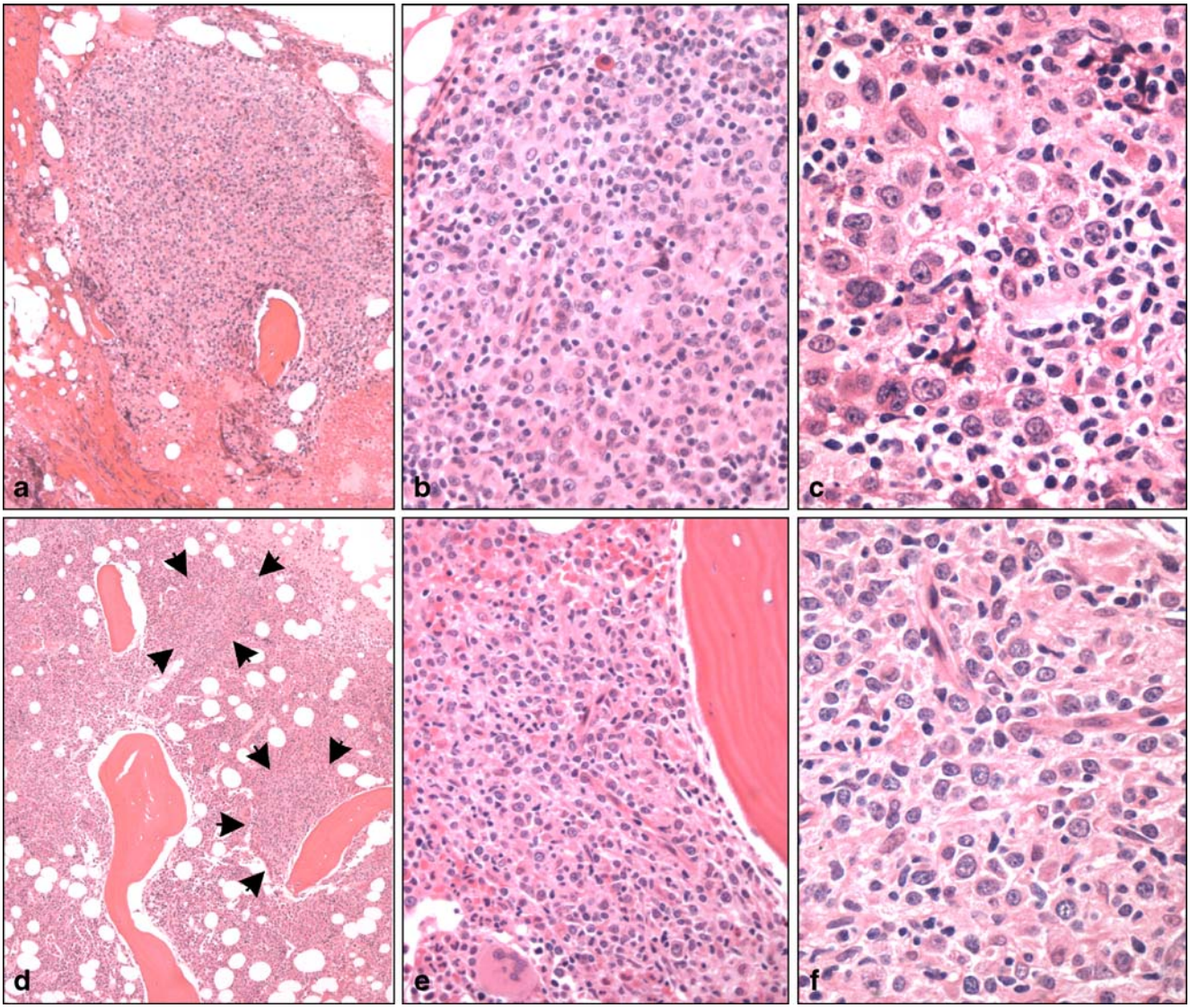

Fig. 1 EBV+ DLBCL of the elderly involving the BM in a nodular pattern (case number 7). **a** BM shows a well-defined paratrabecular nodular infiltrate, clearly visible at low magnification (H&E, 40×). **b** The polymorphic cell population including histiocytes, small lymphocytes, and intermixed neoplastic cells is demonstrated at intermediate magnification (H&E, 200×), while **c** high magnification highlights pleomorphic cytology and occasional RS-like cells (H&E, 400×). EBV− DLBCL with a nodular pattern (case number 12). **d** BM biopsy shows less conspicuous nodules delineated by *arrowheads* (H&E, 40×). **e** Intermediate (H&E, 200×) and **f** high magnification (H&E, 400×) images show a high proportion of centroblast-like cells within the nodules

In contrast, nodules of the six EBV− DLBCL had irregular contours in the majority of cases (4/6, 66%; Fig. 1). Only a few admixed histiocytes were noted (10–30% of all cellular elements within the nodules) that were present in similar numbers as the adjacent uninvolved marrow, and two cases had fewer histiocytes within the nodules compared to the uninvolved marrow, imparting a "negative image" (Fig. 4f). The nodules also had a higher number and density of neoplastic cells compared to most of the EBV+ cases (Fig. 1; Table 3). In all EBV− DLBCL, the neoplastic cells comprised at least 50% of the cellular elements, and in the majority (4/6, 66%), large cells comprised >80% of the nodular cellular infiltrate (Fig. 4e). Half of the biopsies (n= 3) showed only interstitial nodules, while the remaining half showed both interstitial and paratrabecular nodules. The neoplastic cells in the majority of cases (5/6, 83%) demonstrated centroblastic morphology; only one (17%) DLBCL had pleomorphic cytology. The numbers of admixed T cells were variable in EBV+, as well as EBV– DLBCL, and most cases showed a predominance of CD8+ T cells. The inverted CD4:CD8 ratio was especially marked in the 2 EBV+ HIV-associated DLBCL (Table 1). None of the nodules showed evidence of follicular dendritic cell meshworks as assessed by immunohistochemical stains for CD21 and CD23.

Table 3 Diffuse large B cell lymphoma involving the bone marrow in a nodular pattern: patient demographics, morphologic features, phenotype, molecular and cytogenetic characteristics, treatment, and outcome

Case no./ sex/age (year)	Etiology (if applicable)	Morphologic features of nodules				Phenotype	EBER	Karyotype	FISH	Clonality (PCR)	Treatment	Outcome
		Size[a]	Location	Neoplastic cell %	Unique features							
1/F/41	HIV+	S	P	20	RS-like cells	Non-GC	+	89–91<4N>,XXXX, 1, der(3)t(1;3)(q21;p13)×2,+ sder(3)t(3;?)(q11;?),−4,+7×2, t(8;14)(q24;q32)×2,−10,+ del(11)(p11),−12,+i(12)(p10), −13,−16,−17,−18,−21×2,+ mar1−4[cp10]/46,XX[7]	ND	C	None	DOD
2/M/63	Post-tx and elderly	L	I	20		Non-GC	+	46,XY[20]	ND	ND	A-based ChemoRx	DOD
3/M/72	Elderly	S	I	20	RS-like cells	Non-GC	+	46,XY,del(3)(q22q24),der (7)add(7)(p22)add(7) (q36)[14]/46,XY[6]	ND	ND	None	DOD
4/M/57	HIV+and elderly	L	P	60	RS-like cells few apoptotic cells	Non-GC	+	46,XY[20]	ND	ND	A-based ChemoRx	DOD
5/F/70	Post-tx and elderly	S & L	P	60	Few apoptotic cells	Non-GC	+	45−46,X,−X,dup(1)(q41q42; q41q42),+6,+add(7)(q36), ins(11;?)(q22.2;?),dup(12) (q15q24.3),−14, add(14) (p11.2)(q32),del(15) (q22q23),+1−2mar[cp17]/ 46,XX[3]	IgH T BCL6 NT MYC NT Tp53 del	C	A-based ChemoRx	PR, 9 months
6/M/3	Post-tx	S	I	80		Non-GC	+	46,XY[20]	IgH NT	C	A-based ChemoRx	CR, 13 months
7/M/68	Elderly	S & L	I & P	30	RS-like cellsangiocentric with coagulative necrosis	Non-GC	+	46,XY[20]	IgH NT BCL2 NT BCL6 NT c-MYC NT	Poly	Non-A ChemoRx	DOD
8/F/83	Elderly	S & L	I & P	20		Non-GC	+	45,X,−X,t(14;19)(q32;q13) [15]/46,XX[1]	IgH T	C	Non-A ChemoRx	Unknown
9/M/68		S & L	I	80	Nodules devoid of histiocytes	GC	−	ND	ND	ND	A-based ChemoRx	DOD
10/M/51		S & L	I & P	80		GC	−	46, XY[20]	ND	ND	A-based ChemoRx	DOD
11/M/51		S & L	I	80	Nodules devoid of histiocytes	Non-GC	−	51–52,XY,+add(X)(q22),+ add(1))p13,+der(1)t(1;?) (p12;?),+3,+7,t(8;14)(q24; q32), del(15)(q11q21),+ 18,+21[cp20]	ND	ND	A-based ChemoRx	CR, 43 months
13/F/34		S	I & P	50		GC	−	97–101,<4N>,XX,−X,−X,t (3;14)(q27;q32)×2,+t(3;14) (q27;q32),add(6)(q13)×2, del(7)(p14)×2,+hsr(7)(q22)×2,+ i(7)(q10)hsr(7)(q22),−8,add(9)	IgH T BCL6 T BLIMP1 del	C	A-based ChemoRx	CR, 21 mo

14/F/84	S & L	I & P	80	RS-like cells	Non-GC	–	49–51,XX,−2,−5,+1–7mar [cp3]/46,XX[18]	IgH NT BCL6 NT	C	Non-A ChemoRx	DOD
							(p21)×2,+10,−11,−12×2,-15,-17× 2,+18×4, add(19)(q13)×2,+20, + del(20)(q11.2)×2,+1–7mar,+ r(?)×4[cp8]/46,XX[12]				

[a] Please refer to the results section for the parameters used to determine size of nodules

F female, *M* male, *HIV* human immunodeficiency virus, *Post-tx* post solid organ transplant, *S* small, *L* large, *I* interstitial, *P* paratrabecular, *RS* Reed-Sternberg, *GC* germinal center, *Poly* polyclonal, *C* clonal, *T* translocation present, *NT* no translocation detected, *ND* not done, *A-based ChemoRx* anthracycline-based chemotherapy, *non-A ChemoRx* chemotherapy without anthracycline, *CR* complete response, *PR* partial response, *DOD* died of disease

In 11 of 14 (79%) cases, corresponding LN or tissue biopsies were available. Of the seven cases of EBV+ DLBCL available for review, four occurred at extranodal sites (two gastrointestinal tract, one liver, and one kidney), while three were LN-based (one axillary, one mediastinal, and one cervical). Four cases showed variable areas of a polymorphic infiltrate, comprising histiocytes, plasma cells, and small-sized reactive lymphocytes with scattered neoplastic cells being the minority component (Fig. 2a). The two PTLD cases were of the monomorphic type, and the LNs showed near total effacement by sheets of large neoplastic lymphocytes, one had pleomorphic neoplastic cells (Fig. 2i), while the other displayed plasmacytoid features. Overall, pleomorphic neoplastic cells were seen in five cases, and numerous anaplastic or RS-like cells were seen in the majority (4/7, 57%) of cases, similar to findings in the BM biopsies (Fig. 2c). Four of the six EBV− DLBCL, with tissue biopsies available for review, were equally distributed between those occurring at extranodal sites (one testes and one retroperitoneal mass) and LNs (one axillary and one cervical). All these cases displayed centroblastic morphology. As in the corresponding BM biopsies, only a minimal infiltrate of admixed histiocytes was observed. One of the two EBV− nodular BM DLBCL, without available tissue biopsies, demonstrated pleomorphic morphology.

All DLBCL expressed one or more B lineage antigens (CD20, PAX5, OCT2) (Table 1). All EBV+ DLBCL (n=8) were EBER+ by in situ hybridization and had non-GC phenotypes, while two of six (33%) and four of six (66%) EBV– DLBCL had non-GC and GC phenotypes, respectively (Table 3). The neoplastic cells of EBV+ DLBCL more commonly expressed CD30 compared to EBV– DLBCL (7/8, 88% versus 1/6, 17%; P=0.016317; Fig. 4d). All EBV– DLBCL were fascin-negative, while only one of eight (12%) EBV+ DLBCL showed weak fascin staining. Six of eight (75%) EBV+ DLBCL had a type II viral latency pattern (LMP1+ and EBNA2−), and two cases (25%) displayed type III latency (LMP1+ and EBNA2+), both of the latter were PTLDs. In the latter, the number of EBER+ cells was greater than the EBNA2+ and LMP1+ cells combined, and nonoverlapping EBNA2+, and LMP1+ subsets were also seen, consistent with the presence of cell populations with different, as well as transitional, EBV latency types. None of the cases showed any staining for LANA.

Cytogenetic analysis

In 12 of 14 (86%) cases, either BM aspirates or LN/soft tissue biopsies were submitted for cytogenetic analysis. Of these, seven cases had abnormal karyotypes, and all but one exhibited a complex karyotype (Table 3). The most

common cytogenetic aberrations were rearrangements of *IGH* (14q32) detected in five cases (71%). Two cases (one EBV+ and one EBV−), both with non-GC phenotypes, showed t(8;14)(q24;q32) indicative of balanced reciprocal translocations involving *IGH* and *c-MYC*. One EBV+ DLBCL showed t(14;19)(q32;q13) involving *IGH*, and the region encoding *BCL3* and one EBV− DLBCL demonstrated t(3;14)(q27;q32) confirmed to represent a translocation involving *IGH* and *BCL6*. An EBV− DLBCL showed rearrangement of *IGH* only detected by FISH; however, due to the complexity of the karyotype, the partner could not be determined (FISH excluded *BCL6* and *c-MYC*).

Immunoglobulin heavy chain gene rearrangement

In seven of 14 (50%) cases, PCR analysis for *IGH* variable region gene rearrangement was performed, and clonal products were detected in six of seven (86%) cases (Table 3).

Discussion

Bone marrow involvement by DLBCL is less common than low grade B-NHL and occurs in 8–35% of cases [2, 3, 8–13]. However, EBV-associated DLBCL, which represent a small subset of DLBCL (8–12%) [10, 20–24] were shown to have a slightly greater proclivity for the BM (39%) in a recent study [10], compared to EBV − DLBCL. Similar to low grade B-NHLs, different morphologic patterns of BM involvement by DLBCL have been described, which include a predominant or near exclusive presence of diffuse (15–50%), paratrabecular (0–53%), nodular (0–23%), or single cell (17–24%) infiltrates of neoplastic cells [2, 4–6, 13, 16]. Similar patterns and frequencies of marrow involvement by DLBCL were also observed in our series. We decided to focus on DLBCL with a pure nodular pattern in this study since little is known about the phenotypic and clinical spectrum of such cases. A nodular pattern of BM infiltration was noted in 25% of all our cases with BM involvement by DLBCL, and although both EBV− and EBV+ cases were observed, the latter predominated. Of interest, among all cases of EBV+ DLBCL with BM involvement, the vast majority (89%) exhibited a nodular pattern, and EBV+ nodular DLBCL were exclusively seen in patients with documented (organ transplantion, HIV infection) or presumed (old age) immune dysfunction. Differences in the morphologic, phenotypic, and clinical characteristics of EBV+ and EBV– DLBCL with a nodular pattern of BM infiltration were also noted.

EBV+ nodular DLBCL had distinctive morphologic features. The nodules were well circumscribed, and the neoplastic cells usually represented a minor component scattered within a heterogenous population of nonneoplastic inflammatory cells, including histiocytes in most cases. Pleomorphic cytology was quite common, and RS-like cells were observed in 50% of cases. In contrast, the nodules of EBV− DLBCL had more irregular contours, and centroblast-like neoplastic cells comprised the major cellular component in the majority of cases. Lymph node and soft tissue biopsies of the EBV+ DLBCL displayed features similar to those observed in the BM with at least some areas demonstrating neoplastic cells scattered within a polymorphic nonneoplastic background, while all LN biopsies of EBV− DLBCL evaluated showed diffuse infiltrates of centroblast-like cells, similar to what is seen in routine cases of DLBCL.

All EBV+ and one third of the EBV− DLBCL had non-GC phenotypes, and a significant number of EBV+ DLBCL showed CD30 expression by at least a proportion of neoplastic cells compared to EBV − DLBCL, in agreement with prior studies [22, 25]. Staining for fascin, a protein involved in the formation of dendritic processes that is expressed by RS cells in virtually all cases of classical Hodgkin lymphoma (CHL) [26], and approximately 50% of anaplastic large cell lymphomas [27], was seen in the BM and corresponding LN biopsy in only one (13%) of our EBV+ DLBCL, similar to the frequency reported previously [27]. Previous studies of EBV+ DLBCL in PTLD patients have shown high frequencies (36–64%) of type III latency profiles [28, 29]. Lower frequencies of this latency type have been reported in HIV patients (41–50%) [30, 31]. All, except two of the EBV+ cases in our series, displayed type II latency. Both PTLDs, which were of the monomorphic subtype (DLBCL), exhibited type III latency profiles, but populations of cells with different latency types were seen in these cases, similar to previous observations [28, 29]. Our three cases of EBV+ DLBCL of the elderly (see below) showed type II latency, which is the more common latency profile described in these lymphomas [23, 25]. Type III

Fig. 2 EBV+ DLBCL of the elderly (case number 8). An area showing neoplastic lymphocytes scattered in a polymorphic nonneoplastic background in the **a** LN (H&E, 200×) with a similar pattern in the **b** corresponding bone marrow biopsy (H&E, 400×). EBV+ DLBCL of the elderly (case number 3). Markedly pleomorphic neoplastic and RS-like cells in the **c** LN (H&E, 200×) and **d** corresponding bone marrow biopsy (H&E, 400×). EBV+ DLBCL of the elderly (case number 7). A diffuse infiltrate of large neoplastic cells is evident in the **e** LN (H&E, 200×) while the **f** corresponding BM biopsy exhibits angiocentricity with cellular debris and coagulative necrosis (H&E, 400×). EBV+ DLBCL in an HIV patient (case number 4). A high proportion of neoplastic cells are present in the **g** LN (H&E, 200×) and **h** corresponding bone marrow biopsy (H&E, 400×). EBV+ DLBCL in a PTLD patient (case number 2). Sheets of neoplastic cells consistent with monomorphic type of PTLD (DLBCL) are seen in the **i** LN (H&E, 200×), the **j** corresponding BM biopsy shows a moderate infiltrate of nonneoplastic cellular elements (H&E, 400×) ▶

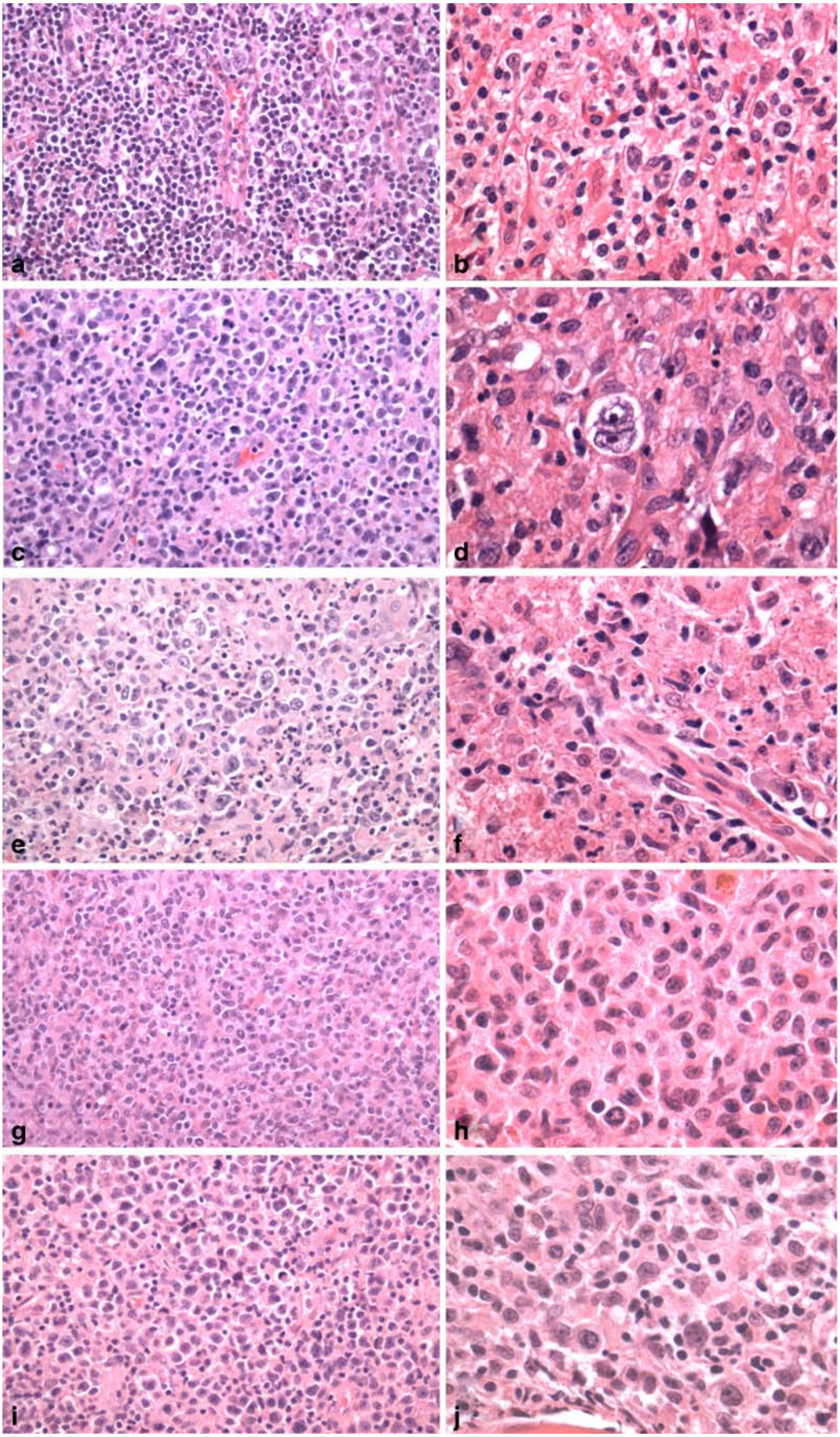
a
b
c
d
e
f
g
h
i
j

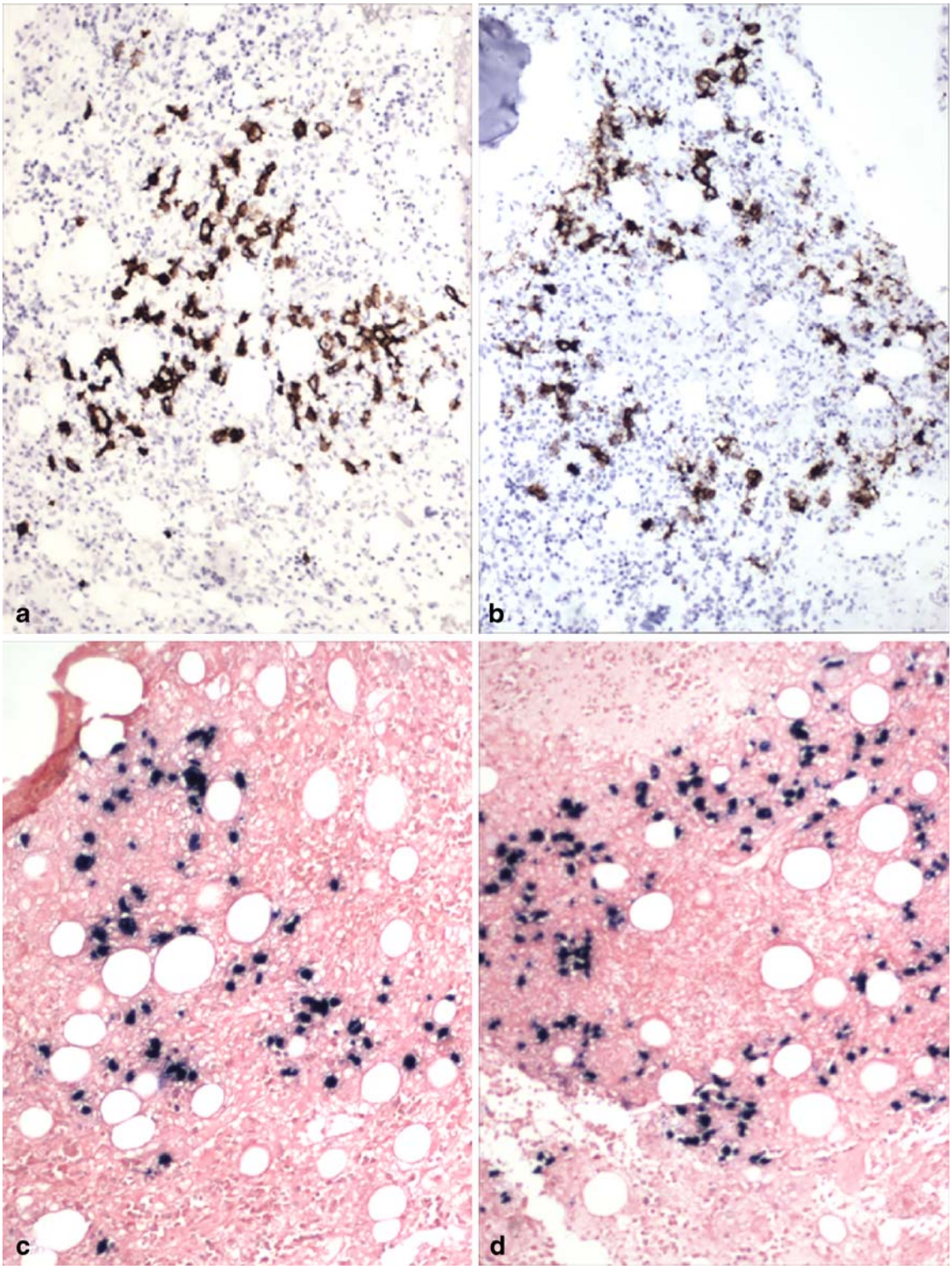

Fig. 3 Distribution patterns of CD20+ and EBER+ neoplastic cells within nodules in the bone marrow biopsies in cases of EBV+ DLBCL (100×). Neoplastic cells are scattered throughout the nodules (**a**, **c**) or seen in a targetoid pattern at the periphery of the nodule (**b**, **d**)

latency has, however, been described in a small proportion of such cases (14–36%) [12, 20, 22, 23, 25, 32].

An interesting finding in our study relates to the presence of EBV+ DLBCL that fulfill the criteria of the recently recognized entity termed EBV+ DLBCL of the elderly [15, 23, 32, 33]. The current World Health Organization classification defines these lymphomas as those occurring in patients >50 years old without any known predisposing

immunodeficiency [15, 23, 32, 33]. A recent survey of EBV-associated lymphomas by Cho et al. described 29 patients with EBV+ DLBCL, 24 of whom were elderly or had a prior history of hepatitis B or C virus infection, tuberculosis, or CHL, suggesting decreased immunity associated with old age and/or environmental cofactors as contributors to lymphomagenesis [20]. It is thought that age associated immune dysfunction, a phenomenon described as "immune senescence," predisposes older individuals to EBV+ lymphomas [34]. Similarities of EBV+ DLBCL of the elderly to B-NHL arising in immunodeficient or immunocompromised patients have been previously described, including a propensity for extranodal disease and the morphologic spectrum of lymphoproliferations, ranging from polymorphic lymphomas resembling polymorphic PTLDs to large cell monomorphic lymphomas indistinguishable from conventional DLBCL [12, 15, 20, 23, 25, 32, 33, 35, 36]. Although, BM involvement has been documented in EBV+ DLBCL of the elderly, to the best of our knowledge, the patterns of BM involvement have not been described. It remains to be seen whether a nodular pattern is the most prevalent pattern of BM involvement in this entity, as seen in our study. Virtually, all prior studies of EBV+ DLBCL have been reported from Asia, whereas, all our three patients were Caucasian and of European descent. Moreover, in contrast to the Asian experience, our cases did not show extranodal involvement.

The morphologic and phenotypic features of our nodular DLBCL also showed an overlap with other types of B cell malignancies, which include T cell/histiocyte-rich large B cell lymphoma (THRLBCL), especially the micronodular variant [37], lymphomatoid granulomatosis (LG), and CHL. Bone marrow involvement, although rare in some of these entities, has been described [38, 39]. The paucity of neoplastic cells and the presence of a polymorphic background, often rich in histiocytes and small reactive T cells, in all these entities, can pose a diagnostic challenge, especially, when reviewing BM biopsies. T cell/histiocyte-rich large B cell lymphomas are usually EBV−; however, rare cases of EBV+ THRLBCL with CD30+ neoplastic cells showing RS-like morphology have been described [40]. However, by definition, the diagnosis of THRLBCL requires the presence of at least a 90% component of nonneoplastic cells, without any aggregates or sheets of large neoplastic cells [15]. All our DLBCL, though rich in nonneoplastic cells, had clusters and/or sheets of neoplastic cells that comprised at least 20% of all cellular elements of the nodules of EBV+ DLBCL and >50% of the EBV− DLBCL. Lymphomatoid granulomatosis also has a polymorphic infiltrate with variable numbers of large EBV+ lymphocytes that may also express CD30. However, these lymphoproliferations show angiocentricity and/or angiodestruction and although occasional bizarre lymphocytes may be seen, classic RS-like cells are infrequent [15]. Angiocentricity and angiodestruction with associated coagulative necrosis was observed focally in only one BM biopsy of our EBV+ DLBCL, within a nodular aggregate that had a large proportion of neoplastic cells. Nodal involvement, which is rare in LG, is usually characterized by a predominance of small-sized T cells in the background, while the LN biopsy of the aforementioned case showed a diffuse infiltrate of predominantly large neoplastic cells, and there was no evidence of extranodal disease arguing against the possibility of LG [41]. Classical Hodgkin lymphoma often presents as nodular polymorphic lymphohistiocytic infiltrates with infrequent CD30+ RS-like cells in the BM [42]. RS cells in CHL coexpress CD30 and CD15 in the majority of cases (80%), are uniformly positive for fascin, and although a minority can express bright CD20 (30%), they usually do not express OCT2 or PU-1 [15, 26]. The CD30+ RS-like cells in our EBV+ DLBCL were uniformly negative for CD15, expressed CD20 in the majority of cases (88%), expressed PU-1 in 50%, and fascin was only expressed in one case. Moreover, all except one case tested, showed clonal immunoglobulin gene rearrangements, which are less commonly detected in CHL by the current assays. The morphologic and phenotypic features of one of our EBV+ cases was similar to the so-called mediastinal gray zone lymphomas, although there was no evidence of mediastinal disease and the latter tend to be EBV− [43]. Methotrexate-related lymphoproliferative disorders can also display similar features, but none of our patients received methotrexate therapy [44]. Although, even nonneoplastic disorders (especially infectious mononucleosis) could morphologically mimic the findings we describe, involvement of the bone marrow is exceptionally rare in these situations. Our study highlights the utility of an extensive immunophenotypic panel, examination of tissue from other sites, and correlation with the clinical features in order to distinguish between these different diagnostic considerations when a nodular pattern of DLBCL is encountered in BM biopsies.

Cytogenetic analysis demonstrated complex cytogenetic aberrations in approximately 50% of our EBV+ and EBV− DLBCL evaluated, but recurrent cytogenetic abnormalities were not observed. Translocations involving *IGH* (14q32) were the most frequently encountered abnormality, detected in almost half of the cases with cytogenetic abnormalities; however, the partners varied. Translocations of *IGH* and *c-MYC* were detected in one case each of EBV+ and EBV− DLBCL. Both had complex karyotypes and non-GC phenotypes, effectively ruling out a diagnosis of Burkitt lymphoma. Intriguingly, an EBV+ DLBCL showed a t(14;19)(q32;q13) on karyotypic analysis, potentially involving the *BCL3* locus, which has been previously reported in a variety of B-NHLs [45]; however, FISH was not performed to confirm involvement of *BCL3* in this case.

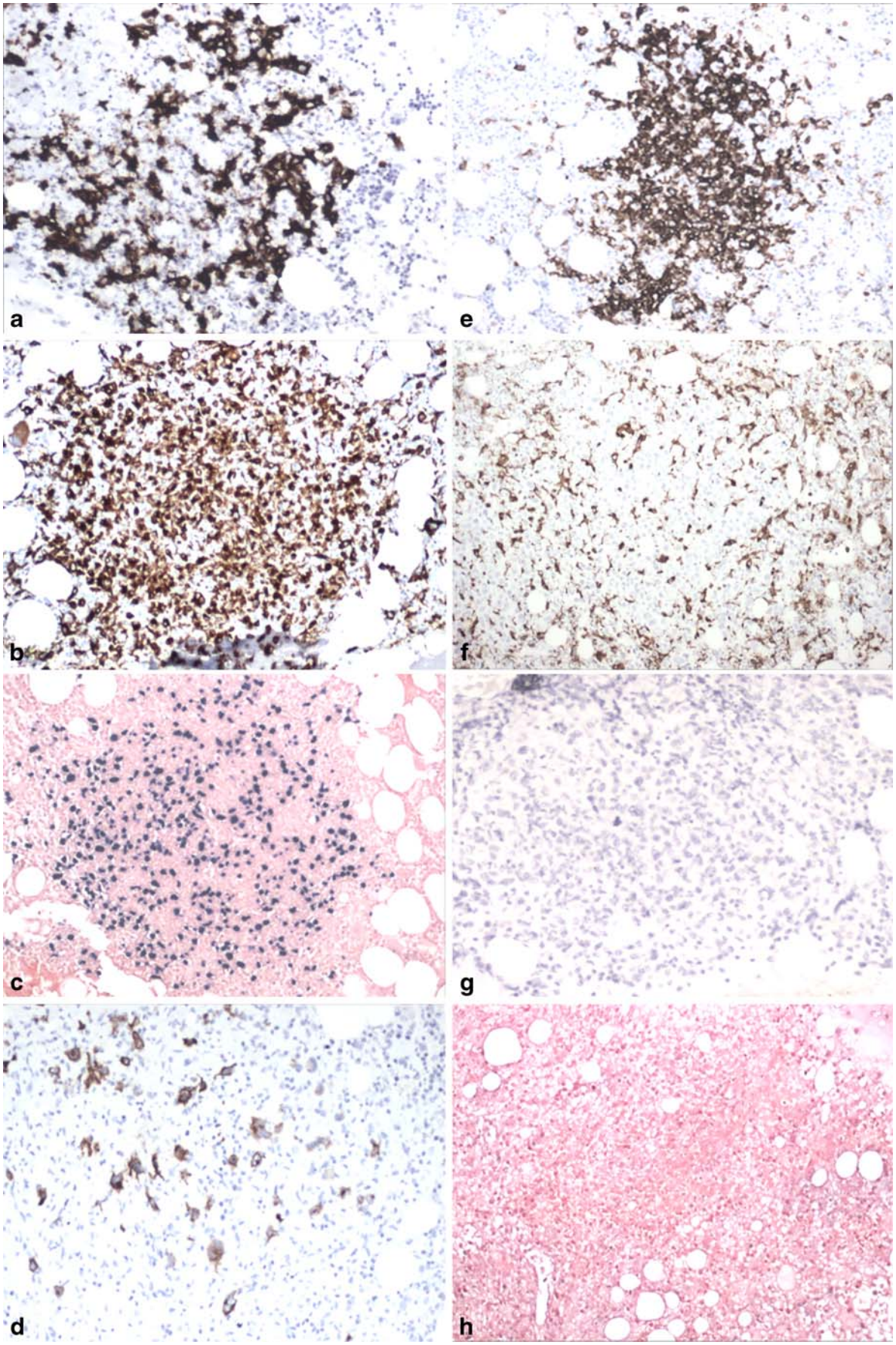
a
e
b
f
c
g
d
h

Cytogenetic findings have not been previously described in surveys of EBV+ DLBCL of the elderly. Our results suggest that the spectrum of cytogenetic aberrations in these cases might be similar to conventional DLBCL [46]. All, but one of our cases, showed clonal IgH gene rearrangement products by PCR analysis. Addition of PCR assays for Ig light chains might have increased the yield of our clonal cases, since cases have been described that show clonality only on using light chain (IgK) primers [47].

Lastly, but importantly, our study suggests investigation of the patient's immune status and evaluation for EBV infection if one observes a nodular pattern of BM involvement by DLBCL with the described features. Determination of EBV status is clinically relevant as multiple studies have demonstrated that EBV+ DLBCL patients have significantly lower overall survival rates, compared to individuals with EBV– DLBCL [10, 22, 24, 33]. We did not see any significant difference in ECOG status, LDH levels, IPI, or clinical outcomes between EBV+ and EBV– DLBCL patients, which might be attributable to our small sample size and/or selection of patients with advanced stage disease (BM involvement). High mortality was seen in both groups, and the small number of patients precludes any assessment of the type of therapy. Since immunosuppressed patients with T cell dysfunction are at risk for "reactivation" of EBV and subsequent development of EBV-associated lymphoproliferative disorders, viral load monitoring in patients with EBV+ PTLDs is performed to detect early disease recurrence and response to treatment [48, 49]. EBV viral load assessment performed in five of our patients at diagnosis of EBV+ B-NHL, which included individuals with PTLD, HIV associated DLBCL, and EBV– DLBCL of the elderly, showed evidence of viral reactivation. Future studies need to investigate the utility of serial serologic or EBV viral load monitoring, as performed in PTLD patients, in detecting early disease recurrence in EBV+ DLBCL of the elderly. Clinical trials using targeted therapies that induce the lytic form of infection in EBV+ lymphoid malignancies in conjunction with gancyclovir treatment have shown promising results [50]. This strategy might also be useful in treating EBV+ DLBCL of the elderly. Since altered lymphocyte development and function contribute to immunosenescence in the elderly, recently proposed treatment approaches aimed at rejuvenating the immune system and augmenting innate immunity in the elderly might be alternative therapeutic options [51].

◀ **Fig. 4** Immunohistochemical studies of the bone marrow (100×). Case number 7 (EBV+ DLBCL), **a** Scattered CD20+ neoplastic B cells representing less than 50% of all cells within the nodule. **b** The nodule is rich in histiocytes (PGM1); **c** neoplastic cells express EBER; and **d** many are CD30+. In contrast, case number 12 (EBV− DLBCL), **e** has numerous CD20+ neoplastic cells within the nodules and **f** fewer histiocytes (PGM1); **g** EBER is negative; and **h** the neoplastic cells do not express CD30

Conflict of interest statement We declare that we have no conflict of interest.

References

1. Wilder RB, Rodriguez MA, Medeiros LJ et al (2002) International prognostic index-based outcomes for diffuse large B-cell lymphomas. Cancer 94:3083–3088
2. Arber DA, George TI (2005) Bone marrow biopsy involvement by non-Hodgkin's lymphoma: frequency of lymphoma types, patterns, blood involvement, and discordance with other sites in 450 specimens. Am J Surg Pathol 29:1549–1557
3. Conlan MG, Bast M, Armitage JO et al (1990) Bone marrow involvement by non-Hodgkin's lymphoma: the clinical significance of morphologic discordance between the lymph node and bone marrow. Nebraska Lymphoma Study Group. J Clin Oncol 8:1163–1172
4. Bartl R, Hansmann ML, Frisch B et al (1988) Comparative histology of malignant lymphomas in lymph node and bone marrow. Br J Haematol 69:229–237
5. McKenna RW, Hernandez JA (1988) Bone marrow in malignant lymphoma. Hematol Oncol Clin North Am 2:617–635
6. Schmid C, Isaacson PG (1992) Bone marrow trephine biopsy in lymphoproliferative disease. J Clin Pathol 45:745–750
7. Kremer M, Quintanilla-Martinez L, Nahrig J et al (2005) Immunohistochemistry in bone marrow pathology: a useful adjunct for morphologic diagnosis. Virchows Arch 447:920–937
8. Campbell J, Seymour JF, Matthews J et al (2006) The prognostic impact of bone marrow involvement in patients with diffuse large cell lymphoma varies according to the degree of infiltration and presence of discordant marrow involvement. Eur J Haematol 76:473–480
9. Hodges GF, Lenhardt TM, Cotelingam JD (1994) Bone marrow involvement in large-cell lymphoma. Prognostic implications of discordant disease. Am J Clin Pathol 101:305–311
10. Park S, Lee J, Ko YH et al (2007) The impact of Epstein–Barr virus status on clinical outcome in diffuse large B-cell lymphoma. Blood 110:972–978
11. Yamauchi A, Fujita S, Ikeda J et al (2007) Diffuse large B-cell lymphoma in the young in Japan: a study by the Osaka Lymphoma Study Group. Am J Hematol 82:893–897
12. Ohshima K, Suzumiya J, Tasiro K et al (1996) Epstein–Barr virus infection and associated products (LMP, EBNA2, vIL-10) in nodal non-Hodgkin's lymphoma of human immunodeficiency virus-negative Japanese. Am J Hematol 52:21–28
13. Foucar K (2001) Bone marrow pathology. ASCP, Chicago
14. Foucar K, McKenna RW, Frizzera G et al (1982) Bone marrow and blood involvement by lymphoma in relationship to the Lukes–Collins classification. Cancer 49:888–897
15. Swerdlow SH, Campo E, Harris NL et al (eds) (2008) WHO classification of tumours of haematopoietic and lymphoid tissues. IARC, Lyon
16. Jeong SY, Chang YH, Lee JK et al (2007) Incidence and histologic patterns of bone marrow involvement of malignant lymphoma based on the World Health Organization classification: a single institution study. Korean J Lab Med 27:383–387
17. Hans CP, Weisenburger DD, Greiner TC et al (2004) Confirmation of the molecular classification of diffuse large B-cell

lymphoma by immunohistochemistry using a tissue microarray. Blood 103:275–282
18. Shaffer LG (2005) An international system for human cytogenetic nomenclature. Karger, Basel
19. Pasqualucci L, Compagno M, Houldsworth J et al (2006) Inactivation of the PRDM1/BLIMP1 gene in diffuse large B cell lymphoma. J Exp Med 203:311–317
20. Cho EY, Kim KH, Kim WS et al (2008) The spectrum of Epstein–Barr virus-associated lymphoproliferative disease in Korea: incidence of disease entities by age groups. J Korean Med Sci 23:185–192
21. Hummel M, Anagnostopoulos I, Korbjuhn P et al (1995) Epstein–Barr virus in B-cell non-Hodgkin's lymphomas: unexpected infection patterns and different infection incidence in low- and high-grade types. J Pathol 175:263–271
22. Kuze T, Nakamura N, Hashimoto Y et al (2000) The characteristics of Epstein–Barr virus (EBV)-positive diffuse large B-cell lymphoma: comparison between EBV(+) and EBV(−) cases in Japanese population. Jpn J Cancer Res 91:1233–1240
23. Oyama T, Yamamoto K, Asano N et al (2007) Age-related EBV-associated B-cell lymphoproliferative disorders constitute a distinct clinicopathologic group: a study of 96 patients. Clin Cancer Res 13:5124–5132
24. Yoshino T, Nakamura S, Matsuno Y et al (2006) Epstein–Barr virus involvement is a predictive factor for the resistance to chemoradiotherapy of gastric diffuse large B-cell lymphoma. Cancer Sci 97:163–166
25. Shimoyama Y, Yamamoto K, Asano N et al (2008) Age-related Epstein–Barr virus-associated B-cell lymphoproliferative disorders: special references to lymphomas surrounding this newly recognized clinicopathologic disease. Cancer Sci 99:1085–1091
26. Pinkus GS, Pinkus JL, Langhoff E et al (1997) Fascin, a sensitive new marker for Reed-Sternberg cells of hodgkin's disease. Evidence for a dendritic or B cell derivation? Am J Pathol 150:543–562
27. Bakshi NA, Finn WG, Schnitzer B et al (2007) Fascin expression in diffuse large B-cell lymphoma, anaplastic large cell lymphoma, and classical Hodgkin lymphoma. Arch Pathol Lab Med 131:742–747
28. Shaknovich R, Basso K, Bhagat G et al (2006) Identification of rare Epstein–Barr virus infected memory B cells and plasma cells in non-monomorphic post-transplant lymphoproliferative disorders and the signature of viral signaling. Haematologica 91:1313–1320
29. Vakiani E, Basso K, Klein U et al (2008) Genetic and phenotypic analysis of B-cell post-transplant lymphoproliferative disorders provides insights into disease biology. Hematol Oncol 26:199–211
30. Delecluse HJ, Hummel M, Marafioti T et al (1999) Common and HIV-related diffuse large B-cell lymphomas differ in their immunoglobulin gene mutation pattern. J Pathol 188:133–138
31. Hamilton-Dutoit SJ, Rea D, Raphael M et al (1993) Epstein–Barr virus-latent gene expression and tumor cell phenotype in acquired immunodeficiency syndrome-related non-Hodgkin's lymphoma. Correlation of lymphoma phenotype with three distinct patterns of viral latency. Am J Pathol 143:1072–1085
32. Oyama T, Ichimura K, Suzuki R et al (2003) Senile EBV+B-cell lymphoproliferative disorders: a clinicopathologic study of 22 patients. Am J Surg Pathol 27:16–26
33. Shimoyama Y, Oyama T, Asano N et al (2006) Senile Epstein–Barr virus-associated B-cell lymphoproliferative disorders: a mini review. J Clin Exp Hematop 46:1–4
34. Ouyang Q, Wagner WM, Walter S et al (2003) An age-related increase in the number of CD8+ T cells carrying receptors for an immunodominant Epstein–Barr virus (EBV) epitope is counteracted by a decreased frequency of their antigen-specific responsiveness. Mech Ageing Dev 124:477–485
35. Tao J, Wasik MA (2001) Epstein–Barr virus associated polymorphic lymphoproliferative disorders occurring in nontransplant settings. Lab Invest 81:429–437
36. Nador RG, Chadburn A, Gundappa G et al (2003) Human immunodeficiency virus (HIV)-associated polymorphic lymphoproliferative disorders. Am J Surg Pathol 27:293–302
37. Dogan A, Burke JS, Goteri G et al (2003) Micronodular T-cell/histiocyte-rich large B-cell lymphoma of the spleen: histology, immunophenotype, and differential diagnosis. Am J Surg Pathol 27:903–911
38. Robak T, Kordek R, Urbanska-Rys H et al (2006) High activity of rituximab combined with cladribine and cyclophosphamide in a patient with pulmonary lymphomatoid granulomatosis and bone marrow involvement. Leuk Lymphoma 47:1667–1669
39. Skinnider BF, Connors JM, Gascoyne RD (1997) Bone marrow involvement in T-cell-rich B-cell lymphoma. Am J Clin Pathol 108:570–578
40. Lim MS, Beaty M, Sorbara L et al (2002) T-cell/histiocyte-rich large B-cell lymphoma: a heterogeneous entity with derivation from germinal center B cells. Am J Surg Pathol 26:1458–1466
41. Takiyama A, Nishihara H, Tateishi U et al (2008) CNS lymphomatoid granulomatosis with lymph node and bone marrow involvements. Neuropathology 28:640–644
42. Franco V, Tripodo C, Rizzo A et al (2004) Bone marrow biopsy in Hodgkin's lymphoma. Eur J Haematol 73:149–155
43. Traverse-Glehen A, Pittaluga S, Gaulard P et al (2005) Mediastinal gray zone lymphoma: the missing link between classic Hodgkin's lymphoma and mediastinal large B-cell lymphoma. Am J Surg Pathol 29:1411–1421
44. Kamel OW, Weiss LM, van de Rijn M et al (1996) Hodgkin's disease and lymphoproliferations resembling Hodgkin's disease in patients receiving long-term low-dose methotrexate therapy. Am J Surg Pathol 20:1279–1287
45. Martin-Subero JI, Ibbotson R, Klapper W et al (2007) A comprehensive genetic and histopathologic analysis identifies two subgroups of B-cell malignancies carrying a t(14;19)(q32;q13) or variant BCL3-translocation. Leukemia 21:1532–1544
46. Dave BJ, Nelson M, Pickering DL et al (2002) Cytogenetic characterization of diffuse large cell lymphoma using multi-color fluorescence in situ hybridization. Cancer Genet Cytogenet 132:125–132
47. van Dongen JJ, Langerak AW, Bruggemann M et al (2003) Design and standardization of PCR primers and protocols for detection of clonal immunoglobulin and T-cell receptor gene recombinations in suspect lymphoproliferations: report of the BIOMED-2 Concerted Action BMH4-CT98–3936. Leukemia 17:2257–2317
48. Cohen JI (2000) Epstein–Barr virus infection. N Engl J Med 343:481–492
49. Tsai DE, Douglas L, Andreadis C et al (2008) EBV PCR in the diagnosis and monitoring of posttransplant lymphoproliferative disorder: results of a two-arm prospective trial. Am J Transplant 8:1016–1024
50. Perrine SP, Hermine O, Small T et al (2007) A phase 1/2 trial of arginine butyrate and ganciclovir in patients with Epstein–Barr virus-associated lymphoid malignancies. Blood 109:2571–2578
51. Dorshkind K, Montecino-Rodriguez E, Signer RA (2009) The ageing immune system: is it ever too old to become young again? Nat Rev Immunol 9:57–62